Model independent analysis for B anomalies

Farvah Mahmoudi[1,2,*], Tobias Hurth[3], Diego Martínez Santos[4], and Siavash Neshatpour[5]

[1] *Université de Lyon, Université Claude Bernard Lyon 1, CNRS/IN2P3, Institut de Physique des 2 Infinis de Lyon, UMR 5822, F-69622, Villeurbanne, France*
[2] *CERN, Theoretical Physics Department, CH-1211 Geneva 23, Switzerland*
[3] *PRISMA+ Cluster of Excellence and Institute for Physics (THEP), Johannes Gutenberg University, D-55099 Mainz, Germany*
[4] *Instituto Galego de Física de Altas Enerxías, Universidade de Santiago de Compostela, Spain*
[5] *INFN-Sezione di Napoli, Complesso Universitario di Monte S. Angelo, Via Cintia Edificio 6, 80126 Napoli, Italy*

Abstract. We discuss the implications of $b \to s\ell^+\ell^-$ measurements and their deviations with respect to the Standard Model predictions in a model-independent framework. We highlight in particular the impact of the recent updated measurements including the updated $B_s \to \phi\mu^+\mu^-$ branching ratios and angular observables, the recent CMS measurement of the branching ratio of $B_s \to \mu^+\mu^-$, and the LHCb measured lepton flavour universality violating ratios $R_{K^0_S}$ and $R_{K^{*+}}$. In addition, we check the compatibility of the new physics effect for the theoretically clean observables with the rest of the neutral B decays observables.

1 Introduction

In the last few years, since the measured deviation in the angular observable P_5' of the $B \to K^*\mu^+\mu^-$ decay [1], there have been several measurements in neutral B-decays indicating tension with the Standard Model (SM). Updated measurements by LHCb for the $P_5'(B \to K^*\mu^+\mu^-)$ have persistently shown tension with the SM which can be explained with short distance new physics (NP) contributions [2, 3]. This is also the case of the overall $B \to K^*\mu^+\mu^-$ angular observables and is supported in addition (see e.g. [4]) by the angular analysis of its isospin partner in the recent measurement of $B^+ \to K^{*+}\mu^+\mu^-$ [5]. The $B_s \to \phi\mu^+\mu^-$ branching fraction [6–8] also indicates tensions with the SM and is measured to be below the SM prediction. This trend is seen in several other $b \to s\ell^+\ell^-$ branching fractions such as $B \to K\mu^+\mu^-$ [9] and $\Lambda_b \to \Lambda\mu^+\mu^-$ [10]. Since the branching fractions are dependent on the relevant local form factors, they suffer from large theoretical uncertainties. In contrast, the angular observables have a reduced sensitivity to the form factor uncertainties, but they are still dependent on the non-local hadronic contributions whose size are not fully known in QCD factorisation. Consequently the significance of the anomalies are dependent on the estimated size of the non-local effects. Recent theoretical progress for a better control of these effects can be found in Refs. [11–13].

A set of observables to test lepton flavour universality violation (LFUV) in $b \to s\ell^+\ell^-$ transitions is defined as $R_H = (B \to H\mu^+\mu^-)/(B \to He^+e^-)$ with $H = K^+, K^*, \phi, ...$ [14]. Unlike the observables mentioned in the previous paragraph, these ratios are very precisely known in the SM. There have been signs of deviation from the SM in the LFUV ratios for the case of R_K [15–17] and R_{K^*} [18]. The recent measurements of $R_{K^0_S}$ and $R_{K^{*+}}$ [19] although within 2σ of the SM prediction, show the same trend as their isospin partners with the central values below the SM predictions. Incidentally, there have also been a slight sign of LFUV in flavour changing neutral current processes in the Kaon sector [20] (currently the ex-

* e-mail: nazila@cern.ch

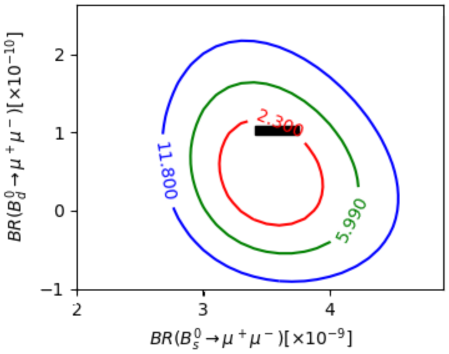

Figure 1. Two dimensional likelihood plot of $\mathrm{BR}(B_{s,d} \to \mu^+\mu^-)$.

perimental uncertainty is quite large for these processes).

The significance of each of the B-anomalies, individually is around $\sim 2-3\sigma$, however collectively they can be explained by common NP scenarios and have a much larger significance in a global analysis [21–26].

Another precisely predicted observable with an uncertainty of less than 5% in its SM prediction is $\mathrm{BR}(B_s \to \mu^+\mu^-)$ which has been measured by several experiments. Previous measurements of ATLAS [27], CMS [28] and LHCb [29, 30] were in about 2σ tension with the SM prediction [21]. However, the situation has changed with the recent data from CMS [31]. For our fits, we combined the ATLAS [27] and LHCb [29, 30] results together with the recent CMS [31] measurement, considering a joint 2D likelihood as shown in Fig 1. We obtained the experimental combined value of the $B_s \to \mu^+\mu^-$ branching ratio to be

$$\mathrm{BR}(\mathrm{B_s} \to \mu^+\mu^-)^{\mathrm{comb.}}_{\mathrm{exp}} = \left(3.52^{+0.32}_{-0.30}\right) \times 10^{-9}\,, \quad (1)$$

which is within 1σ of the SM prediction.

2 Coherence of clean observables with the rest of the rare *B*-decay observables

In order to examine the consistency of the implication of the clean observables for new physics as compared to the rest of the observables [32, 33], we perform two sets of fits; one to the clean observables where we consider R_K, R_{K^*} as well as their isospin partners $R_{K_S^0}$ and $R_{K^{*+}}$ [19] and also $\mathrm{BR}(B_{s,d} \to \mu^+\mu^-)$, and another one considering the rest of the $bs\ell\ell$ observables. The observable calculations and the χ^2 fitting is done using the SuperIso public program [34–38].

2.1 Clean observables

In table 1 we give the one-dimensional NP fits to clean observables and compare them with our 2021 fit results [21]. Compared to Ref. [21], we now include the two LFUV ratios $R_{K_S^0}$ and $R_{K^{*+}}$ [19] as well as the R_K measurement by Belle [39] in the [1,6] GeV^2 bin and the updated combination for $\mathrm{BR}(B_s \to \mu^+\mu^-)$ as given in Eq. (1).

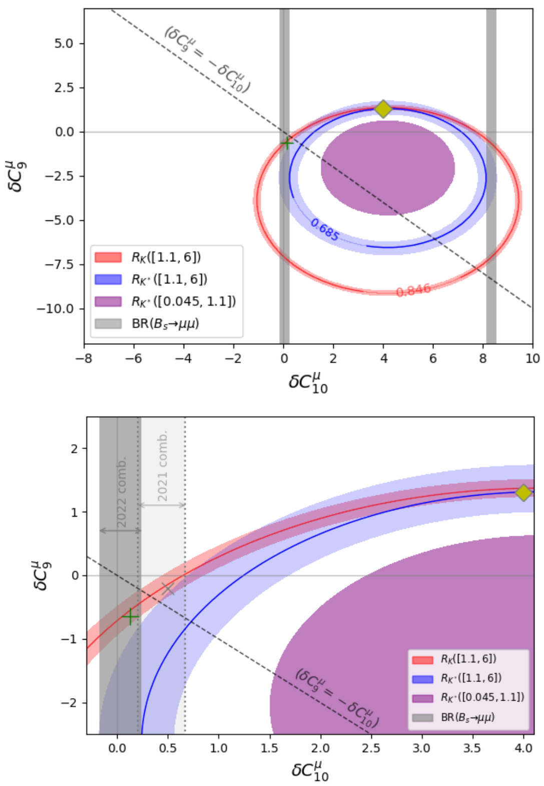

Figure 2. The prediction of $R_{K^{(*)}}$ and $\mathrm{BR}(B_s \to \mu^+\mu^-)$ within $1\sigma\left(=\sqrt{\sigma^2_{\mathrm{th}}+\sigma^2_{\mathrm{exp}}}\right)$ of their measured values. On the lower plot we have the zoomed-in version of the upper plot. The dark gray band indicates the 1σ region corresponding to the updated combination of $\mathrm{BR}(B_s \to \mu\mu)$ and the lighter gray region (on the lower plot) with the dotted borders corresponds to the 2021 combination. The yellow diamond indicates the best fit value to $R_{K^{(*)}}$, while the green plus sign (gray cross) corresponds to the best fit point when the 2022 (2021) combination for $\mathrm{BR}(B_s \to \mu\mu)$ is included in the fit.

Only LFUV ratios and $B_{s,d} \to \ell^+\ell^-$ **2021 fit results** ($\chi^2_{\rm SM} = 28.19$)			
	b.f. value	$\chi^2_{\rm min}$	$\rm Pull_{SM}$
δC_9	-1.00 ± 6.00	28.1	0.2σ
δC_9^e	0.80 ± 0.21	11.2	4.1σ
δC_9^μ	-0.77 ± 0.21	11.9	4.0σ
δC_{10}	0.43 ± 0.24	24.6	1.9σ
δC_{10}^e	-0.78 ± 0.20	9.5	4.3σ
δC_{10}^μ	0.64 ± 0.15	7.3	4.6σ
$\delta C_{\rm LL}^e$	0.41 ± 0.11	10.3	4.2σ
$\delta C_{\rm LL}^\mu$	-0.38 ± 0.09	7.1	4.6σ

Only LFUV ratios and $B_{s,d} \to \ell^+\ell^-$ **2022 fit results** ($\chi^2_{\rm SM} = 30.63$)			
	b.f. value	$\chi^2_{\rm min}$	$\rm Pull_{SM}$
δC_9	-2.00 ± 5.00	30.5	0.4σ
δC_9^e	0.83 ± 0.21	10.8	4.4σ
δC_9^μ	-0.80 ± 0.21	11.8	4.3σ
δC_{10}	0.03 ± 0.20	30.6	0.1σ
δC_{10}^e	-0.81 ± 0.19	8.7	4.7σ
δC_{10}^μ	0.50 ± 0.14	16.2	3.8σ
$\delta C_{\rm LL}^e$	0.43 ± 0.11	9.7	4.6σ
$\delta C_{\rm LL}^\mu$	-0.33 ± 0.08	12.4	4.3σ

Table 1. Comparison of the fits to clean observables with the 2021 fit results [21] on the left and the updated 2022 fits on the right.

All observables except LFUV ratios and $B_{s,d} \to \ell^+\ell^-$ **2021 fit results** ($\chi^2_{\rm SM} = 200.1$)			
	b.f. value	$\chi^2_{\rm min}$	$\rm Pull_{SM}$
δC_9	-1.01 ± 0.13	158.2	6.5σ
δC_9^e	0.70 ± 0.60	198.8	1.1σ
δC_9^μ	-1.03 ± 0.13	156.0	6.6σ
δC_{10}	0.34 ± 0.23	197.7	1.5σ
δC_{10}^e	-0.50 ± 0.50	199.0	1.0σ
δC_{10}^μ	0.41 ± 0.23	196.5	1.9σ
$\delta C_{\rm LL}^e$	0.33 ± 0.29	198.9	1.1σ
$\delta C_{\rm LL}^\mu$	-0.75 ± 0.13	167.9	5.7σ

All observables except LFUV ratios and $B_{s,d} \to \ell^+\ell^-$ **2022 fit results** ($\chi^2_{\rm SM} = 221.8$)			
	b.f. value	$\chi^2_{\rm min}$	$\rm Pull_{SM}$
δC_9	-0.95 ± 0.13	185.1	6.1σ
δC_9^e	0.70 ± 0.60	220.5	1.1σ
δC_9^μ	-0.96 ± 0.13	182.8	6.2σ
δC_{10}	0.29 ± 0.21	219.8	1.4σ
δC_{10}^e	-0.60 ± 0.50	220.6	1.1σ
δC_{10}^μ	0.35 ± 0.20	218.7	1.8σ
$\delta C_{\rm LL}^e$	0.34 ± 0.29	220.6	1.1σ
$\delta C_{\rm LL}^\mu$	-0.64 ± 0.13	195.0	5.2σ

Table 2. Comparison of the fits to all observables except the clean ones with the 2021 fit results on the left and the updated 2022 fits on the right.

While the significance of NP in $C_9^{e,\mu}$ or C_{10}^e has slightly increased, the C_{10}^μ solution is now less favoured compared to the 2021 results [21]. This is expected as the new combination of $\text{BR}(B_s \to \mu^+\mu^-)$ is now in much better agreement with the SM prediction and constrains more C_{10}^μ. The inclusion of $\text{BR}(B_s \to \mu^+\mu^-)$ in this set of observables is crucial in breaking the degeneracy between NP in δC_9^μ and δC_{10}^μ for explaining the measured values of the LFUV ratios as can be clearly seen in figure 2 where without $\text{BR}(B_s \to \mu^+\mu^-)$ the best fit point of $R_{K^{(*)}}$ is given by the yellow diamond while including it moves the best fit value to the green plus sign. The impact of the updated value of the $\text{BR}(B_s \to \mu^+\mu^-)$ can bee seen in the lower plot by comparing the green plus sign with the gray cross corresponding to the best fit point when the 2021 combination for $\text{BR}(B_s \to \mu^+\mu^-)$ was considered.

2.2 All except the clean observables

We consider now the 1-dimensional NP fits to the rest of the observables, excluding the LFUV ratios and $B_{s,d} \to \ell^+\ell^-$. We assume 10% power correction for the non-factorisable contributions beyond QDC factorisation [40–43]. Compared to Ref. [21] we use the updated LHCb results for the $B_s \to \phi\mu^+\mu^-$ observables [7, 8] with 8.4 fb^{-1} of data. The CMS measurement for $F_H(B^+ \to K^+\mu^+\mu^-)$ [44] and the LHCb measurement of the angular observables of $B \to K^* e^+ e^-$ [45] have also been considered. As can be seen in table 2, the hierarchy of the preferred NP contributions is similar to the 2021 results, where the most preferred scenarios are still NP in lepton flavour violating δC_9^μ and NP in lepton flavour universal δC_9 with the third most preferred description given by NP in the chiral basis $\delta C_{\rm LL}^\mu$. The above mentioned scenarios however are showing a $\sim 0.4\sigma$ reduced significance compared to our 2021 results which is mainly due to the updated $B_s \to \phi\mu^+\mu^-$ experimental data.

For the fit to all observables except the clean ones there is no significant indication for NP within the electron sector since not only the measurements in the electron sector are in good agreement with their SM predictions, there are also far less data compared to the decays with muons. Comparing the result of table 2 with the result of the previous subsection (table 1) we see that there is not a full agreement for the preferred scenarios, however, there are common scenarios such as NP contributions to δC_9^μ [46, 47] which have a large significance for both datasets with best fit points that agree within 1σ.

The compatibility of the two-dimensional NP fits to "clean observables" and the NP fits to "all observables except the clean ones" can be seen in figure 3 where also the significant impact of including or removing $\mathrm{BR}(B_s \to \mu^+\mu^-)$ from each dataset is clearly visible, especially for the clean observables.

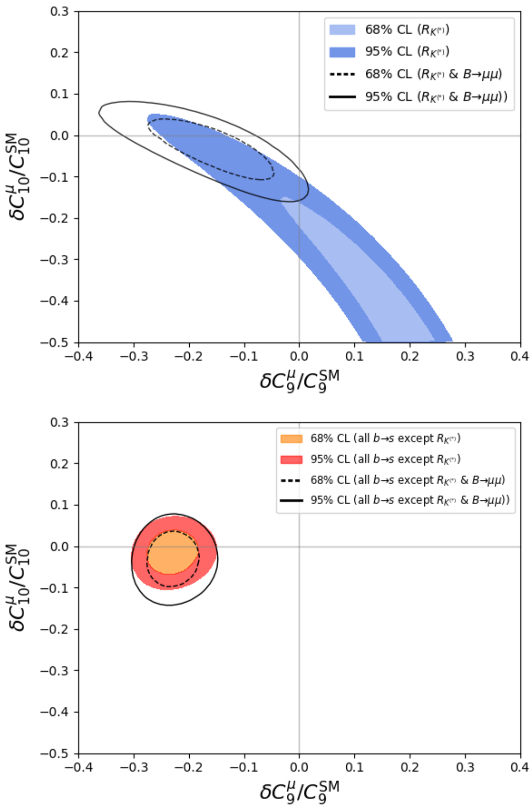

Figure 3. Two-dimensional fits to the clean observables (top) and to the rest of the observables (bottom).

3 Global fits to all $b \to s\ell^+\ell^-$ observables

For a global analysis of the NP implications of rare B-decays, we need to take into account all relevant $b \to s$ decays combining the datasets of section 2.1 and section 2.2. We assume 10% error for the power corrections when applicable.

3.1 One- and two-dimensional fits

The 1-dim NP fits to the rare B-decays are given in table 3. As anticipated from the comparison of the fits to clean observables and the rest of the observables, the most favoured scenario to explain the overall data is lepton flavour violating NP in δC_9^μ. The other prominent scenarios are NP in $\delta C_{\rm LL}^\mu$ followed by lepton flavour universal NP in δC_9. While the hierarchy of the favoured scenarios has not changed, it should be noted that NP in δC_{10}^μ is now less favoured which is mostly due to the updated combination for $\mathrm{BR}(B_s \to \mu^+\mu^-)$. This can also be seen in the decrease of the significance of δC_{LL}^μ compared to the 2021 fit results. The decrease of preference of NP in δC_{10}^μ can also be seen in the 2-dim fits of figure 4.

In the 1-and 2-dim fits of table 3 and figure 4 we have not shown the NP fits to the radiative coefficient δC_7, the scalar and pseudoscalar coefficients ($\delta C_{Q_{1,2}}$) or the coefficients where the hadronic currents are right-handed ($\delta C_i'$) since they are all strongly constrained by data. The situation can in principle change when several coefficients can simultaneously contribute, this is clearly the case when doing a simultaneous fit to δC_{10}^μ and $\delta C_{Q_{1,2}}^\mu$ [48] which would otherwise be severely constrained by $\mathrm{BR}(B_s \to \mu^+\mu^-)$ if only one single coefficient would contribute.

3.2 Multidimensional fit

A multidimensional fit gives in principle a more realistic picture than assuming new physics contribution to only a single coefficient, as it is very unlikely for a UV-complete scenario to merely affect one coefficient while the rest of the coefficients are kept to their SM values. Therefore, here we consider a 20-dim fit varying all relevant Wilson coefficients (table 4). Besides being more realistic, this multidimensional fit has the advantage of avoiding the look elsewhere effect (LEE) since LEE not only takes place when one makes a selected choice of observables but is also relevant in the case when a posteriori a subset of specific NP directions are

All observables 2021 fit results ($\chi^2_{\rm SM} = 225.8$)			
	b.f. value	$\chi^2_{\rm min}$	$\rm Pull_{SM}$
δC_9	-0.99 ± 0.13	186.2	6.3σ
δC_9^e	0.79 ± 0.20	207.7	4.3σ
δC_9^μ	-0.95 ± 0.12	168.6	7.6σ
δC_{10}	0.32 ± 0.18	222.3	1.9σ
δC_{10}^e	-0.74 ± 0.18	206.3	4.4σ
δC_{10}^μ	0.55 ± 0.13	205.2	4.5σ
$\delta C_{\rm LL}^e$	0.40 ± 0.10	206.9	4.3σ
$\delta C_{\rm LL}^\mu$	-0.49 ± 0.08	180.5	6.7σ

All observables 2022 fit results ($\chi^2_{\rm SM} = 253.5$)			
	b.f. value	$\chi^2_{\rm min}$	$\rm Pull_{SM}$
δC_9	-0.95 ± 0.13	215.8	6.1σ
δC_9^e	0.82 ± 0.19	232.4	4.6σ
δC_9^μ	-0.92 ± 0.11	195.2	7.6σ
δC_{10}	0.08 ± 0.16	253.2	0.5σ
δC_{10}^e	-0.77 ± 0.18	230.6	4.8σ
δC_{10}^μ	0.43 ± 0.12	238.9	3.8σ
$\delta C_{\rm LL}^e$	0.42 ± 0.10	231.4	4.7σ
$\delta C_{\rm LL}^\mu$	-0.43 ± 0.07	213.6	6.3σ

Table 3. Comparison of the fits to all observables with the 2021 fit results on the left and the updated 2022 fits on the right.

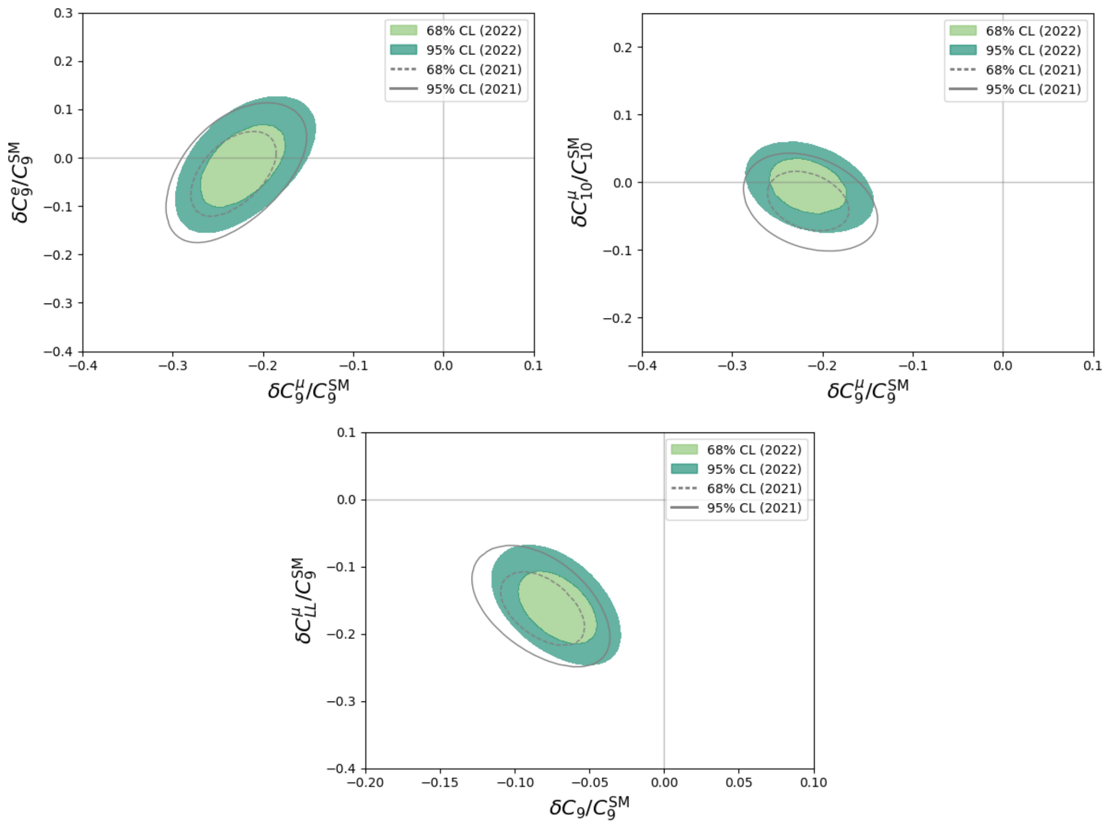

Figure 4. Two-dimensional fit to all rare B-decay observables.

assumed which is circumvented when all possible Wilson coefficients are varied. With a large set of free parameters and the limited decay modes there can be flat directions or non-sensitive NP coefficients that can be removed by considering the correlations and likelihood profiles in order to get an "effective" number of degrees of freedom ($\rm dof_{eff}$). In the 20-dim fit we find degeneracy in δC_{10}^e and $\delta C_{10}^{e\prime}$ which results in having $\rm dof_{eff} = 19$. With the current data, there are still several of the Wilson coefficients which are only loosely constrained, especially in the electron sector where there is less

All observables with $\chi^2_{\rm SM} = 225.8$, nr. obs.= 173 **2021 fit results** ($\chi^2_{\rm min} = 151.6$; Pull$_{\rm SM} = 5.5(5.6)\sigma$)			
δC_7		δC_8	
0.05 ± 0.03		-0.70 ± 0.40	
$\delta C_7'$		$\delta C_8'$	
-0.01 ± 0.02		0.00 ± 0.80	
δC_9^μ	δC_9^e	δC_{10}^μ	δC_{10}^e
-1.16 ± 0.17	-6.70 ± 1.20	0.20 ± 0.21	degenerate w/ $\downarrow$
$\delta C_9'^\mu$	$\delta C_9'^e$	$\delta C_{10}'^\mu$	$\delta C_{10}'^e$
0.09 ± 0.34	1.90 ± 1.50	-0.12 ± 0.20	degenerate w/ $\uparrow$
$\delta C_{Q_1}^\mu$	$\delta C_{Q_1}^e$	$\delta C_{Q_2}^\mu$	$\delta C_{Q_2}^e$
0.04 ± 0.10	-1.50 ± 1.50	-0.09 ± 0.10	-4.10 ± 1.5
$\delta C_{Q_1}'^\mu$	$\delta C_{Q_1}'^e$	$\delta C_{Q_2}'^\mu$	$\delta C_{Q_2}'^e$
0.15 ± 0.10	-1.70 ± 1.20	-0.14 ± 0.11	-4.20 ± 1.2

All observables with $\chi^2_{\rm SM} = 253.5$, nr. obs.= 183 **2022 fit results** ($\chi^2_{\rm min} = 179.1$; Pull$_{\rm SM} = 5.5(5.5)\sigma$)			
δC_7		δC_8	
0.06 ± 0.03		-0.80 ± 0.40	
$\delta C_7'$		$\delta C_8'$	
-0.01 ± 0.01		-0.30 ± 1.30	
δC_9^μ	δC_9^e	δC_{10}^μ	δC_{10}^e
-1.14 ± 0.19	-6.50 ± 1.90	0.21 ± 0.20	degenerate w/ $\downarrow$
$\delta C_9'^\mu$	$\delta C_9'^e$	$\delta C_{10}'^\mu$	$\delta C_{10}'^e$
0.05 ± 0.32	1.40 ± 2.30	-0.03 ± 0.19	degenerate w/ $\uparrow$
$\delta C_{Q_1}^\mu$	$\delta C_{Q_1}^e$	$\delta C_{Q_2}^\mu$	$\delta C_{Q_2}^e$
0.04 ± 0.20	-1.60 ± 1.70	-0.15 ± 0.08	-4.10 ± 0.9
$\delta C_{Q_1}'^\mu$	$\delta C_{Q_1}'^e$	$\delta C_{Q_2}'^\mu$	$\delta C_{Q_2}'^e$
-0.03 ± 0.20	-1.50 ± 2.10	-0.16 ± 0.08	-4.00 ± 1.2

Table 4. Comparison of 20-dim fit to all observables with the 2022 (2021) result on the right (left). The Pull$_{\rm SM}$ in the parenthesis is given for dof$_{\rm eff}$ = 19.

data. The significance of the NP in our 20-dim fit is 5.5σ, remaining the same as what we had found in Ref. [21].

4 Conclusions

We presented the NP fits to rare B decays which include the recent measurements of $B_s \to \phi\mu^+\mu^-$ observables and the lepton flavour violating ratios $R_{K^{*+}}$ and R_{K_S} by LHCb. We have furthermore updated the BR($B_s \to \mu^+\mu^-$) combination to include the very recent measurement by CMS. The main change in the NP fits is a reduction for the significance of a δC_{10}^μ solution or the scenarios involving it which is mainly due to the recent BR($B_s \to \mu^+\mu^-$) measurement being in agreement with the SM value. However, the hierarchy of the favoured scenarios for the global fit has remained stable and the preferred scenario is still NP with δC_9^μ. We also updated our twenty dimensional fit which avoids the look elsewhere effect finding a 5.5σ significance.

Acknowledgments

FM is grateful to the FCCP2022 organisers for their invitation to present this work.

References

[1] LHCb collaboration, *Measurement of Form-Factor-Independent Observables in the Decay $B^0 \to K^{*0}\mu^+\mu^-$*, *Phys. Rev. Lett.* **111** (2013) 191801 [1308.1707].

[2] LHCb collaboration, *Angular analysis of the $B^0 \to K^{*0}\mu^+\mu^-$ decay using 3 fb^{-1} of integrated luminosity*, *JHEP* **02** (2016) 104 [1512.04442].

[3] LHCb collaboration, *Measurement of CP-Averaged Observables in the $B^0 \to K^{*0}\mu^+\mu^-$ Decay*, *Phys. Rev. Lett.* **125** (2020) 011802 [2003.04831].

[4] T. Hurth, F. Mahmoudi and S. Neshatpour, *Model independent analysis of the angular observables in $B^0 \to K^{*0}\mu^+\mu^-$ and $B^+ \to K^{*+}\mu^+\mu^-$*, *Phys. Rev. D* **103** (2021) 095020 [2012.12207].

[5] LHCb collaboration, *Angular Analysis of the $B^+ \to K^{*+}\mu^+\mu^-$ Decay*, *Phys. Rev. Lett.* **126** (2021) 161802 [2012.13241].

[6] LHCb collaboration, *Angular analysis and differential branching fraction of the decay $B_s^0 \to \phi\mu^+\mu^-$*, *JHEP* **09** (2015) 179 [1506.08777].

[7] LHCb collaboration, *Angular analysis of the rare decay $B_s^0 \to \phi\mu^+\mu^-$*, *JHEP* **11** (2021) 043 [2107.13428].

[8] LHCb collaboration, *Branching Fraction Measurements of the Rare $B_s^0 \to \phi\mu^+\mu^-$ and $B_s^0 \to f_2'(1525)\mu^+\mu^-$- Decays*, *Phys. Rev. Lett.* **127** (2021) 151801 [2105.14007].

[9] LHCb collaboration, *Differential branching fractions and isospin asymmetries of $B \to K^{(*)}\mu^+\mu^-$ decays*, *JHEP* **06** (2014) 133

[1403.8044].

[10] LHCb collaboration, *Differential branching fraction and angular analysis of $\Lambda_b^0 \to \Lambda\mu^+\mu^-$ decays*, *JHEP* **06** (2015) 115 [1503.07138].

[11] C. Bobeth, M. Chrzaszcz, D. van Dyk and J. Virto, *Long-distance effects in $B \to K^*\ell\ell$ from analyticity*, *Eur. Phys. J. C* **78** (2018) 451 [1707.07305].

[12] N. Gubernari, D. van Dyk and J. Virto, *Non-local matrix elements in $B_{(s)} \to \{K^{(*)}, \phi\}\ell^+\ell^-$*, *JHEP* **02** (2021) 088 [2011.09813].

[13] N. Gubernari, M. Reboud, D. van Dyk and J. Virto, *Improved Theory Predictions and Global Analysis of Exclusive $b \to s\mu^+\mu^-$ Processes*, 2206.03797.

[14] G. Hiller and F. Kruger, *More model-independent analysis of $b \to s$ processes*, *Phys. Rev. D* **69** (2004) 074020 [hep-ph/0310219].

[15] LHCb collaboration, *Test of lepton universality using $B^+ \to K^+\ell^+\ell^-$ decays*, *Phys. Rev. Lett.* **113** (2014) 151601 [1406.6482].

[16] LHCb collaboration, *Search for lepton-universality violation in $B^+ \to K^+\ell^+\ell^-$ decays*, *Phys. Rev. Lett.* **122** (2019) 191801 [1903.09252].

[17] LHCb collaboration, *Test of lepton universality in beauty-quark decays*, *Nature Phys.* **18** (2022) 277 [2103.11769].

[18] LHCb collaboration, *Test of lepton universality with $B^0 \to K^{*0}\ell^+\ell^-$ decays*, *JHEP* **08** (2017) 055 [1705.05802].

[19] LHCb collaboration, *Tests of lepton universality using $B^0 \to K_S^0\ell^+\ell^-$ and $B^+ \to K^{*+}\ell^+\ell^-$ decays*, *Phys. Rev. Lett.* **128** (2022) 191802 [2110.09501].

[20] G. D'Ambrosio, A.M. Iyer, F. Mahmoudi and S. Neshatpour, *Anatomy of kaon decays and prospects for lepton flavour universality violation*, *JHEP* **09** (2022) 148 [2206.14748].

[21] T. Hurth, F. Mahmoudi, D.M. Santos and S. Neshatpour, *More Indications for Lepton Nonuniversality in $b \to s\ell^+\ell^-$*, *Phys. Lett. B* **824** (2022) 136838 [2104.10058].

[22] M. Algueró, B. Capdevila, S. Descotes-Genon, J. Matias and M. Novoa-Brunet, *$b \to s\ell^+\ell^-$ global fits after R_{K_S} and $R_{K^{*+}}$*, *Eur. Phys. J. C* **82** (2022) 326 [2104.08921].

[23] W. Altmannshofer and P. Stangl, *New physics in rare B decays after Moriond 2021*, *Eur. Phys. J. C* **81** (2021) 952 [2103.13370].

[24] M. Ciuchini, M. Fedele, E. Franco, A. Paul, L. Silvestrini and M. Valli, *Lessons from the $B^{0,+} \to K^{*0,+}\mu^+\mu^-$ angular analyses*, *Phys. Rev. D* **103** (2021) 015030 [2011.01212].

[25] L.-S. Geng, B. Grinstein, S. Jäger, S.-Y. Li, J. Martin Camalich and R.-X. Shi, *Implications of new evidence for lepton-universality violation in $b \to s\ell^+\ell^-$ decays*, *Phys. Rev. D* **104** (2021) 035029 [2103.12738].

[26] F. Mahmoudi, *Theoretical Review of Rare B Decays*, in *20th Conference on Flavor Physics and CP Violation* , 8, 2022 [2208.05755].

[27] ATLAS collaboration, *Study of the rare decays of B_s^0 and B^0 mesons into muon pairs using data collected during 2015 and 2016 with the ATLAS detector*, *JHEP* **04** (2019) 098 [1812.03017].

[28] CMS collaboration, *Measurement of properties of $B_s^0 \to \mu^+\mu^-$ decays and search for $B^0 \to \mu^+\mu^-$ with the CMS experiment*, *JHEP* **04** (2020) 188 [1910.12127].

[29] LHCb collaboration, *Measurement of the $B_s^0 \to \mu^+\mu^-$ decay properties and search for the $B^0 \to \mu^+\mu^-$ and $B_s^0 \to \mu^+\mu^-\gamma$ decays*, *Phys. Rev. D* **105** (2022) 012010 [2108.09283].

[30] LHCb collaboration, *Analysis of Neutral B-Meson Decays into Two Muons*, *Phys. Rev. Lett.* **128** (2022) 041801 [2108.09284].

[31] CMS collaboration, *Measurement of $B_s^0 \to \mu^+\mu^-$ decay properties and search for the $B^0 \to \mu\mu$ decay in proton-proton collisions at $\sqrt{s} = 13$ TeV*, CMS-PAS-BPH-21-006.

[32] T. Hurth, F. Mahmoudi, D. Martinez Santos and S. Neshatpour, *Lepton nonuniversality in exclusive $b \to s\ell\ell$ decays*, *Phys. Rev. D* **96** (2017) 095034 [1705.06274].

[33] A. Arbey, T. Hurth, F. Mahmoudi, D.M. Santos and S. Neshatpour, *Update on the $b \to s$ anomalies*, *Phys. Rev. D* **100** (2019) 015045 [1904.08399].

[34] F. Mahmoudi, *SuperIso: A Program for calculating the isospin asymmetry of $B \to K^*\gamma$ in the MSSM*, *Comput. Phys. Commun.* **178** (2008) 745 [0710.2067].

[35] F. Mahmoudi, *SuperIso v2.3: A Program for calculating flavor physics observables in Supersymmetry*, *Comput. Phys. Commun.* **180** (2009) 1579 [0808.3144].

[36] F. Mahmoudi, *SuperIso v3.0, flavor physics observables calculations: Extension to NMSSM*, *Comput. Phys. Commun.* **180** (2009) 1718.

[37] S. Neshatpour and F. Mahmoudi, *Flavour Physics with SuperIso*, *PoS* **TOOLS2020** (2021) 036 [2105.03428].

[38] S. Neshatpour and F. Mahmoudi, *Flavour Physics Phenomenology with SuperIso*, *PoS* **CompTools2021** (2022) 010 [2207.04956].

[39] BELLE collaboration, *Test of lepton flavor universality and search for lepton flavor violation in $B \to K\ell\ell$ decays*, *JHEP* **03** (2021) 105 [1908.01848].

[40] T. Hurth, F. Mahmoudi and S. Neshatpour, *Implications of the new LHCb angular analysis of $B \to K^*\mu^+\mu^-$: Hadronic effects or new physics?*, *Phys. Rev. D* **102** (2020) 055001 [2006.04213].

[41] V.G. Chobanova, T. Hurth, F. Mahmoudi, D. Martinez Santos and S. Neshatpour, *Large hadronic power corrections or new physics in the rare decay $B \to K^*\mu^+\mu^-$?*, *JHEP* **07** (2017) 025 [1702.02234].

[42] S. Neshatpour, V.G. Chobanova, T. Hurth, F. Mahmoudi and D. Martinez Santos, *Direct comparison of global fits to the $B \to K^*\mu^+\mu^-$ data assuming hadronic corrections or new physics*, in *52nd Rencontres de Moriond on QCD and High Energy Interactions*, pp. 87–90, 2017 [1705.10730].

[43] S. Neshatpour, T. Hurth and F. Mahmoudi, *Searching for New Physics with $B^0 \to K^{*0}\mu^+\mu^-$*, *PoS* **ICHEP2020** (2021), 406 [2012.07408].

[44] CMS collaboration, *Angular analysis of the decay $B^+ \to K^+\mu^+\mu^-$ in proton-proton collisions at $\sqrt{s} = 8$ TeV*, *Phys. Rev. D* **98** (2018) 112011 [1806.00636].

[45] LHCb collaboration, *Strong constraints on the $b \to s\gamma$ photon polarisation from $B^0 \to K^{*0}e^+e^-$ decays*, *JHEP* **12** (2020) 081 [2010.06011].

[46] T. Hurth, F. Mahmoudi and S. Neshatpour, *On the anomalies in the latest LHCb data*, *Nucl. Phys. B* **909** (2016) 737 [1603.00865].

[47] T. Hurth, F. Mahmoudi and S. Neshatpour, *Global fits to $b \to s\ell\ell$ data and signs for lepton non-universality*, *JHEP* **12** (2014) 053 [1410.4545].

[48] A. Arbey, T. Hurth, F. Mahmoudi and S. Neshatpour, *Hadronic and New Physics Contributions to $b \to s$ Transitions*, *Phys. Rev. D* **98** (2018) 095027 [1806.02791].